CrystEngComm

Accepted Manuscript

Journal Name

ARTICLE

Synthesis, electron microscopy and X-ray characterization of oxymagnesite, MgO·2MgCO₃, formed from amorphous magnesium carbonate

S. Frykstrand,[a] C. Strietzel,[a] J. Forsgren,[a] J. Ångström,[b] V. Potin[c] and M. Strømme[a]

Till date, the peculiar compound called oxymagnesite, MgO·2MgCO₃: an intermediate formed during thermal decomposition of hydrated magnesium carbonates, has only been described a handful of times without a distinct description of its formation or morphology. In the current work we present the first scanning and transmission electron microscopy images of an oxymagnesite crystal together with crystallographic data. The oxymagnesite was synthesized in a controlled manner via decomposition of amorphous magnesium carbonates (AMCs) subjected to varying relative humidity. We show that oxymagnesite only is formed when AMC is hydrated above a certain level, which we attribute to a structural inequivalence between CO₃ groups induced by water in AMC subjected to high humidity resulting in a weakening of some of the Mg-CO₃ bonds. The study provides an understanding of the conditions needed for oxymagnesite formation and shows how hydrated AMCs can be used as precursors for different types of magnesium carbonates.

Introduction

Magnesium is one of the most abundant elements in the earth's crust and it can form several types of hydrated and basic carbonates, such as nesquehonite (Mg(HCO₃)(OH)·2H₂O), hydromagnesite (Mg₅(CO₃)₄(OH)₂·4H₂O) and anhydrous magnesite (MgCO₃). Crystalline magnesium carbonates are industrially important materials that can be synthesized in different forms and used in products such as paper and pharmaceutical formulations. Recently, we also reported on the synthesis of an amorphous and mesoporous form of magnesium carbonate[1-3] that can act as a solubility enhancer of poorly soluble drugs.[4] In addition to the different types of magnesium carbonates mentioned above there exists a metastable compound called oxymagnesite (MgO·2MgCO₃). Oxymagnesite is a conspicuous compound that has only been described in a few previous works, most often formed from thermal decomposition of various hydrated magnesium carbonates such as nesquehonite.[5-7] In the decomposition reaction the formation of oxymagnesite has been attributed to the non-equivalent positions for the CO₃ groups in the nesquehonite crystal which allows one third of the CO₃²⁻ anions to loose CO₂ upon thermal treatment at a lower temperature

then the remaining CO₃ groups.[6] Oxymagnesite has also been reported to form from a reaction between Mg(OH)₂ and CO₂ in an anhydrous synthesis[8] and from a solid state reaction of CO₂ and MgO using steam.[9, 10] However, despite the earlier studies, there seems to be no clear understanding regarding the formation of oxymagnesite. The aim of this study was to address this issue by synthesizing oxymagnesite in a controlled way via thermal decomposition of amorphous magnesium carbonates, MgCO₃·xH₂O (AMC), that were hydrated at different relative humidities (RHs). Through the approach used in the current work it was possible to investigate how humidity can be used to produce different forms of AMCs and their corresponding ability to form oxymagnesite upon thermal treatment. In addition to this, a clear description of the morphology and the crystal structure of oxymagnesite are provided.
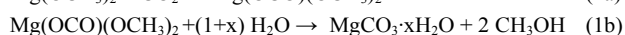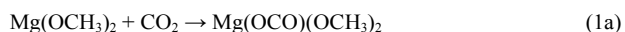
Experimental

Materials

The materials used in the synthesis of oxymagnesite were magnesium methoxide (Mg(OCH₃)₂) (6-10wt% dispersed in methanol, Sigma-Aldrich) and carbon dioxide (CO₂) (N48,

AirLiquid). For the synthesis of magnesite as a reference material mono ethylene glycol (MEG) (99.9%, VWR), sodium chloride (NaCl) (99%, WVR) and hydromagnesite ($Mg_5(CO_3)_4(OH)_2 \cdot 4H_2O$) (< 99%, 3way Pharm) were used. All reagents were used without further purification.

Methods

SYNTHESIS OF HYDRATED AMC:S. Four different AMCs were synthesized according to the following reactions:

$$Mg(OCH_3)_2 + CO_2 \rightarrow Mg(OCO)(OCH_3)_2 \qquad (1a)$$
$$Mg(OCO)(OCH_3)_2 + (1+x) H_2O \rightarrow MgCO_3 \cdot xH_2O + 2 CH_3OH \quad (1b)$$

Synthesis of amorphous hydrated AMC according to reaction 1 has earlier been described by Kornprobst and Plank.[11] They used a 2-fold excess of liquid water in order to hydrolyze the $Mg(OCO)(OCH_3)_2$, (MMMC), while in this work the hydrolysis was carried out using water vapor at different RHs. In the current work the synthesis was carried out as follows:
The $Mg(OCH_3)_2$ solution was heated to 50 °C under a CO_2 pressure of 1.5 bar during 3 hours while being continuously stirred in order to form MMMC. The resulting solution was dried in a rotary evaporator for five hours at 50 °C. The dried powder was divided into five different parts where four of them were placed in dessicators with different RHs. The RH in the dessicators were adjusted to 11, 52, 75 and 100% using supersaturated LiCl, $Mg(NO_3)_2$ and NaCl solutions as well as deionized water, respectively. The samples will henceforward be referred to as A, B, C, and D (see Table 1). Samples A, B and C were kept in their respective desiccator for 48 hours while the corresponding time for sample D was 24 hours since this shorter time was found sufficient for hydrolysis at 100% RH. The fifth sample (denoted sample E) was hydrolyzed in liquid water for ~ 2 hours. All hydrolyzation reactions were carried out at room temperature.
THERMAL TREATMENT OF HYDRATED AMC:S. The AMCs were heat treated at 300 °C for 70 hours in air. As will become obvious from the presented results, this temperature is just below the decomposition temperature for AMC, hence it is possible to isolate oxymagnesite by thermal treatment at this temperature.
SYNTHESIS OF MAGNESITE. Magnesite, used as a reference material in the present study, was synthesized as described earlier.[12] Briefly a 500 ml 95% MEG solution was prepared by adding 25 mg deionized water to 475 mg 99.9% MEG. About 1 mol/kg solvent NaCl was added in order to achieve supersaturation. Subsequently about 10 g hydromagnesite was added to 250 ml of the solution. The resulting solution was then heated to 150 ºC and bubbled with CO_2 gas for 3 days and the resulting precipitate was subsequently washed with both deionized water and ethanol.

Characterization

POWDER X-RAY DIFFRACTION (PXRD) was performed with a Bruker D8 TwinTwin instrument using Cu-K$_\alpha$ radiation. Samples were ground and dispersed in ethanol and applied to a

silicon zero background sample holder prior to analysis. The instrument was set to operate at 45 kV and 40 mA. Analyses of the diffractograms were performed using the software EVA V2.0 from Bruker. Phases analysis of sample E was performed using the Rietveld method[13] implemented in the FullProf program.[14] The background was fitted as a linear interpolation of a set of points because of the complicated background caused by the amorphous phase(s) present in the sample. 54 parameters were refined: 38 background points, the cell parameter a, 5 peak parameters using the Pseudo-Voigt peak function, the position of the C-atom at 8c and the O-atom at 24g (3 parameters), individual isotropic atomic displacement factors for each type of element (3 parameters), the site occupancy of the two O-atom positions (2 parameters), the scale factor and a displacement error.
ATTENUATED TOTAL REFLECTION FOURIER TRANSFORM INFRARED SPECTROSCOPY (ATR-FTIR) was performed with a Bruker Tensor27 instrument using a Platinum ATR diamond cell. A background scan was recorded prior to the measurement and subtracted from the sample spectra, 32 scans were signal-averaged for each spectrum.
SCANNING ELECTRON MICROSCOPY (SEM) was performed using a Leo 1550 instrument equipped with an in-lens detector. Prior to the analysis the samples were sputter coated with a thin layer of gold/palladium.
TRANSMISSION ELECTRON MICROSCOPY (TEM) was performed on sample E using a JEOL 2100 LaB6 microscope operating at 200kV. For observation under the electron microscope, TEM samples were prepared by dropping the sample E dispersed in water onto lacey membrane carbon coated copper grids. The diffraction patterns were stored with a Gatan Erlangshen™ digital camera. The study of the experimental Selected Area Electron Diffraction (SAED) patterns was performed using the Gatan Digital Micrograph software whereas the simulations of SAED patterns were carried out with the Java Electron Microscopy Software.[15]
THERMAL GRAVIMETRIC ANALYSIS (TGA) was carried out under a flow of air in an inert alumina cup with sample sizes of approximately 25 mg in a Thermogravimteric analyser from Mettler Toledo, model TGA/SDTA851e. The samples were heated from room temperature (RT) to 700 °C using a 5 °C/min heating rate. In addition to the TGA measurements the samples were studied using **SIMULTANEOUS DIFFERENCE THERMAL ANALYSIS (SDTA)** with the same instrument. For this analysis approximately 25 mg of sample was put into a alumina sample cup and heated from RT to 300 °C using a 10 °C/min heating rate and at 300 °C the temperature was kept fixed for an additional 10 hours. Prior to the TGA and SDTA analyses the samples were stored at 100 °C for a minimum of 24 hours in order to remove all surface adsorbed water.

Results

Synthesis of AMC, $MgCO_3 \cdot xH_2O$. MMMC was successfully synthesized as confirmed by the IR spectrum of the product, see Fig. 1a where the peaks at 2950, 2885 and 2822 cm^{-1} correspond to vibrations of the OCH$_3$-groups, 1633, 1325, 822,

713 and 626 cm^{-1} to vibrations of the COO-groups, 1450 and 1192 cm^{-1} to vibrations of the CH$_3$-groups and 1097 and 1052 cm^{-1} to vibrations of the CO-groups. The MMMC was subsequently completely hydrolyzed at all RHs employed in the present study and resulted in formation of AMC. Representative IR spectra for samples A, B, C and D can be found in Fig. 1b. In the IR spectra of the hydrolyzed samples the bands at 1440, 1100, 850 and 650 cm^{-1} stem from vibrations of the carbonate groups while the peak at 1640 cm^{-1} and the broad peak at ~ 3200 cm^{-1} stem from water. No signs of methoxyl groups, -OCH$_3$, *i.e.* vibrations at 2830, 2950 and 3000 cm^{-1} could be seen in the samples after hydrolysis which verifies that the hydrolysis was complete for all hydrolyzed samples.
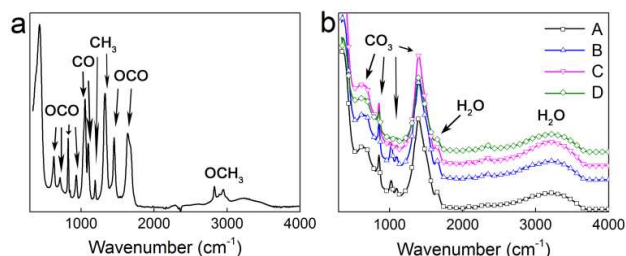

Fig. 1. IR spectra of Mg(OCO)(OCH$_3$)$_2$ before (a) and after (b) hydrolysis. After hydrolysis MgCO$_3$·xH$_2$O, AMC, has been formed.

Thermal treatment of AMC. The phases present in the heat treated samples are summarized in Table 1 and X-ray diffractograms for the different samples can be found in Fig. 2. As evident from the diffractograms oxymagnesite is present in samples C, D and E, and some traces of the compound can also be found in sample B. Samples C, D and E were all subjected to high RH conditions or liquid water during hydrolysis. Only sample E formed oxymagnesite without detectable traces of magnesite or periclase, while samples C and D formed a mixture of magnesite and, in some cases, periclase together with oxymagnesite. Thus, except from sample A, every sample formed oxymagnesite and/or magnesite after the heat treatment.

Table 1. Overview of the samples used in the study.

Sample	RH for hydrolysis (%)	Composition after thermal treatment
A	11	periclase**
B	52	magnesite + traces of oxymagnesite
C	75	oxymagnesite + magnesite + periclase**
D	100	oxymagnesite + magnesite + periclase**
E	hydrolyzed in liquid water	oxymagnesite

* All samples were to various extents still somewhat amorphous after the thermal treatments

** The presence of periclase in some of the samples is believed to be due to differences in temperature for different sample positions inside the furnace
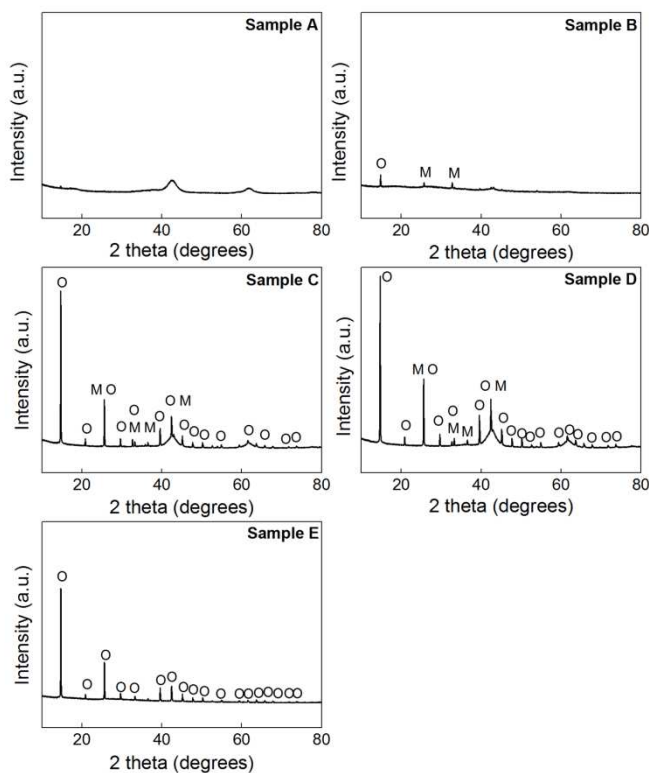

Fig. 2. PXRD patterns for all samples types after thermal treatment. O and M indicate the peak stemming from oxymagnesite and magnesite, respectively.

TGA and SDTA results of AMC. In order to understand why oxymagnesite is formed as a result of thermal treatment only for samples that were exposed to high RHs, samples A, B, C and D were examined with TGA prior to the heat treatment, *i.e.* after reaction step 1b. In order to remove surface adsorbed water, so that the TGA curves only show decompositions due to water associated with the amorphous structure, all samples were stored at 100 °C for at least 24 hours prior to TGA examination. The results of the TGA measurements can be seen in Fig. 3a. The weight of all samples clearly decreases in the temperature region between 150 ºC and 350 ºC. As carbonate decomposition typically happens at temperatures exceeding 350 ºC the loss of weight at these lower temperatures can be ascribed to water being released from the amorphous structure. The presence of water in the different samples prior to heat treatment is further supported by the IR spectra in Fig. 1b where the peaks at 1640 and 3200 cm^{-1} are due to H$_2$O and -OH vibrations, respectively. Although similar in shape, some differences between the samples can be noted, which is especially clear when looking at the derivative of the TGA curves, *i.e.* the dTGA curves in Fig. 3b, in the temperature region between 250 ºC and 350 ºC and in the inset in Fig. 3a where the TGA curves between 250 and 400 °C are highlighted. A weight loss region, slightly above 300 °C can be observed for the samples hydrolyzed at the highest RH values. This weight loss is most distinct for sample D. In the dTGA curves this loss is manifested as an extra peak for samples C and D in addition to the peaks also found for sample A and B.

To further study potential differences between the samples TGA and SDTA data were recorded while the temperature was held at 300 ºC for 5 hours, see Fig 4a and b. From these curves it can be noted that all samples lost weight during the first ~30 minutes before the temperature stabilized at 300 ºC. As discussed earlier this is most likely due to the loss of water from the samples. Interestingly, however, samples C and D (which both form oxymagnesite) exhibit an additional weight loss after approximately 3 hours, Fig. 4a. This weight loss is accompanied by a change in slope in the corresponding SDTA curves, see Fig. 4b.
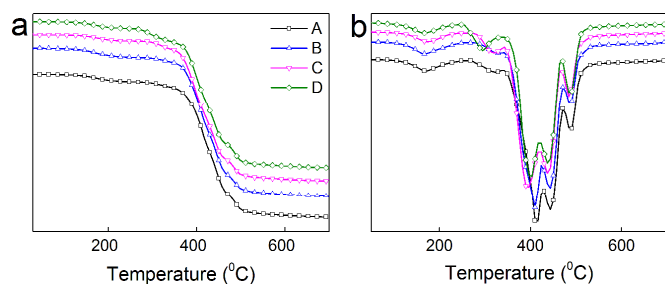

Fig. 3. TGA (a) and dTGA (b) curves for AMC samples formed after hydrolysis. The inset in panel a shows an enlargement of the TGA curves in the temperature region between 250 and 400 °C.
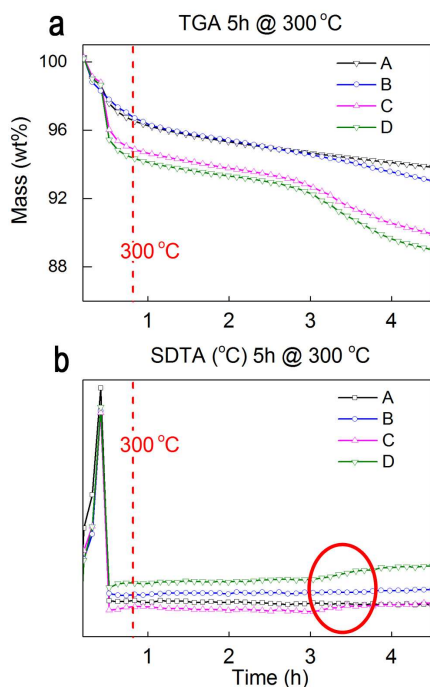

Fig. 4. TGA (a) and SDTA (b) curves for AMC samples after the temperature was set to 300 °C. The vertical dashed lines indicate the time point at which the temperature stabilized at 300 °C after being increased from RT. The red circle in panel b marks the region where a change in the slope of the sample C and D SDTA curves can be detected.

Characterization of oxymagnesite. The structure, morphology and stability of oxymagnesite were characterized using sample E since oxymagnesite was the only crystalline phase present in this sample, see Fig. 2.

SEM and TEM micrographs of the oxymagnesite crystals are shown in Fig. 5a and b, respectively. Evidently oxymagnesite forms rhombic dodecahedral crystals, a couple of hundreds nanometers in diameter, see Fig. 5a and b, which are easily distinguishable from the cubic crystals of magnesite, see Fig. 5c. The TGA measurements performed on oxymagnesite and magnesite (the reference sample) in order to compare the stability of these phases, see Fig. 6, showed that oxymagnesite decomposes at approximately 400 ºC while magnesite decomposes at about 500 ºC.
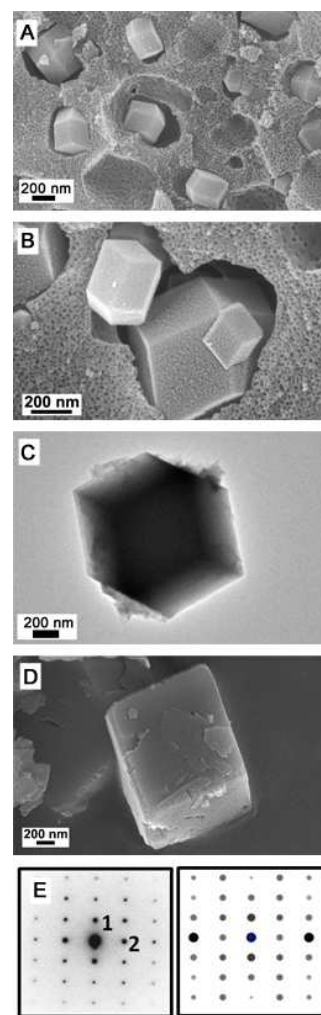

Fig. 5. SEM micrograph of sample E after heat treatment, oxymagnesite crystals can be seen in the amorphous matrix (a and b), TEM micrograph of a sample E oxymagnesite crystal (c) and SEM micrograph of a magnesite crystal (d). Experimental (e, left) and simulated (e, right) SAED patterns obtained from the crystal shown in panel c.
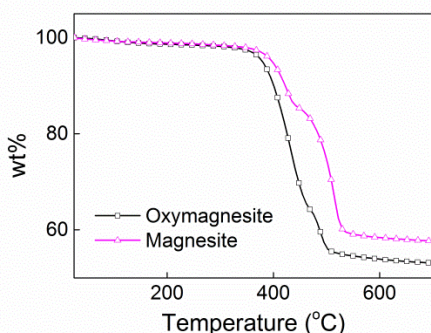
Fig. 6. TGA curves of oxymagnesite and magnesite

The structure, with space group I-43m, a=8.5205(1) and the atomic parameters listed in Table 2, refined from the diffractogram (see Fig. 7), matches the structure reported by Watabe et al.[7] well, except from the fact that the (2 2 0) peak almost disappears during the refinement assuming the low occupancy of the O atom at the 8c site stipulated in this previous work. Instead the occupancies of both O-atom sites were refined resulting in partial occupation of both positions, both about 90% filled. Using these refined occupancies, see Table 2, the composition of the compound would be $Mg_3C_2O_{6.9}$ which is close to the nominal composition of oxymagnesite, $Mg_3C_2O_7$. It is possible that the addition of a preferred orientation may yield a better fit for the occupancies suggested by Watabe et al.;[7] but it is unlikely that crystals embedded in the amorphous matrix would be preferably oriented in some particular direction.

Table 2. Refined atomic parameter of oxymagnesite in sample E

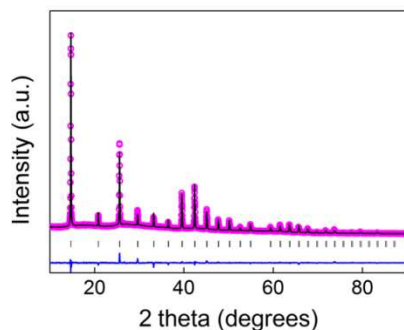| Atom (Wyckoff position)	a	b	c	Site occupancy	B_{iso}
Mg(12d)	0.25	0.5	0	1	3.87(8)
C(8c)	0.2847(4)	0.2847(4)	0.2847(4)	1	1.1(2)
O(24g)	0.4045(3)	0.2242(2)	0.2242(2)	0.915(4)	1.33(8)
O(6b)	0	0.5	0.5	0.907(6)	1.33(8)

Fig. 7. PXRD pattern of sample E (pink circles), refined pattern (continuous black line), the difference between these (continuous blue line) and the refined peak positions (vertical black lines).

Besides PXRD, structure determination was performed with SAED patterns acquisition in the transmission electron microscope. Individual SAED patterns were saved from several individual crystals, similar to the one shown in Fig. 5b. Fig. 5d illustrates a typical SAED experimental pattern with its simulation carried out using the data given in Table 2. The experimental interatomic distances are d_1=0.60 nm and d_2=0.43 nm corresponding to $d_{(10-1)}$=0.602 nm and $d_{(0-20)}$=0.426 nm. This pattern is interpreted as the oxymagnesite structure, with [101] zone axis.

Discussion

Formation of oxymagnesite from hydrated AMCs.

It is clear from the results that it is possible to synthesize oxymagnesite by heat treatment of AMC. However, here oxymagnesite is only formed from AMC when the MMMC have been hydrolyzed in RHs exceeding a certain threshold, which in our work was found to lie in the interval between 11 and 52% at RT. Hladky,[6] who was the first to describe oxymagnesite, observed this phase from a decomposition of nesquehonite. Hladky attributed the formation of oxymagnesite to the non-equivalent crystal sites of the CO_3 groups in nesquehonite allowing one third of the CO_2 in the material to be released prior to the remaining CO_2 upon thermal treatment. In spite of more research following Hladky's work no clear explanation regarding the formation of oxymagnesite exists; however, it has been speculated that the formation of oxymagnesite in solid-gas reactions between $Mg(OH)_2$ and CO_2 under dry or mildly humid carbonation conditions is a result of restructuring between MgO and $MgCO_3$ in the absence of water.[9] Herein oxymagnesite formed from AMC hydrolyzed in high RHs, see Fig. 2 and Table 1.

Based on the results from Hladky[6] and the particular findings presented in Fig. 3 in the present work the formation of oxymagnesite upon thermal treatment of the AMC samples can be explained as follows: The CO_3 groups in the high RH samples C, D and E are structurally non-equivalent with one of three groups forming a weaker bond to the magnesium atom which enables its CO_2 release at a lower temperature that for the other CO_3 groups. In the low RH samples A and B the corresponding bond strength for all CO_3 groups are most likely very similar and they thus release CO_2 at approximately the same temperature preventing oxymagnesite formation.

The structural differences between the samples can be understood by examining the phase diagram for the system $MgO-CO_2-H_2O$ at 25 °C as presented by White,[16] according to which, around atmospheric pressure of CO_2 at 11 and 52% RH, magnesite is the most stable phase while at higher RH, *i.e.* 75 and 100% RH, nesquehonite is the most stable one. Yet, in the present study neither magnesite nor nesquehonite formed upon hydrolysis during 48 hours. It should, however, be mentioned that nesquehonite formed if the hydrolysis was carried out for a longer time, *i.e.* for about five weeks in 100% RH. Despite the lack of observed crystallization, 48 hours was found to be

enough time for all samples to form AMC from MMMC (24 hours was sufficient for sample D). The slow crystallization for magnesium carbonate is likely due to a fundamental barrier preventing Mg^{2+} and CO_3^{2-} ions from forming long-range ordered structures.[17] Concluding from the phase diagram,[16] AMC samples forming oxymagnesite at high RH, *i.e.* sample C, D and E, are in their amorphous state "on their way" to form nesquehonite. Hence, when they decompose, oxymagnesite is formed as an intermediate according to:

$$3MgCO_3 \cdot xH_2O \rightarrow \textbf{MgO} \cdot \textbf{2MgCO}_3 + CO_2 + xH_2O \rightarrow 3MgO + 2CO_2 \quad (2)$$

and if the temperature for the thermal treatment is just below the decomposition temperature it is possible to isolate oxymagnesite.

Structure and stability of the AMC samples.

The dTGA curves for samples C and D exhibit an additional peak compared to those of the lower RH samples, Fig. 3b, corresponding to a TGA weight loss region slightly above 300 °C, Fig. 3a. This indicates a different structural arrangement of the high RH samples as compared to the low RH ones. The fact that sample C and D start to decompose at lower temperatures than the low RH samples shows that the former are structurally weaker. Destabilization of AMC when water is incorporated into the structure has earlier been observed for rehydration of basic magnesium carbonate.[18] Hence, it seems likely that during hydration of AMC water occupies positions that weaken the carbonate bond.

From Fig. 4, where the TGA and corresponding SDTA curves for samples A, B, C and D held at 300 °C are displayed, it may be speculated that the formation of oxymagnesite (sample C and D) occurs after ~3 h. After this time point a faster decrease in mass is observed in the TGA curves for samples C and D (Fig. 4a) while the slopes of the SDTA curves change (red circle in Fig. 4b). The latter is an indication of crystallization.

The role of water in magnesium carbonates has been the subject for many studies.[19-24] For example has the difficulty of precipitating magnesite from an aqueous solution of Mg^{2+} and CO_3^{2-} ions at ambient conditions often been explained by the strong hydration status of the Mg^{2+} ion.[17, 22, 23] Indeed, both experimental and computational studies revealed the presence of a strong inner-sphere hydration shell around Mg^{2+} ions in water that contains six water molecules in an octahedral arrangement and an additional outer shell, composed of up to 12 water molecules, that bonds via hydrogen bonding to the inner sphere.[23-25] The strong Mg^{2+}-water association is rationalized by the high charge density of Mg^{2+} ions resulting from the small ionic radius.[21, 24, 26, 27] Hence, even if magnesite is the most stable phase at all conditions,[19, 28] it has been reported to form only at elevated pressures and temperatures[19, 22, 29-31] or when the activity of the water has been lowered either by salts[19, 22, 28, 32] or by organic molecules like MEG.[12] The relative ease to nucleate hydrous magnesium carbonates in comparison to magnesite has been suggested to be a result of water facilitating the nucleation process by direct incorporation

into the structure[17] which is why hydrated magnesium carbonates are more easily crystallized than magnesite. Additionally, they are also less thermodynamically stable,[19, 28] which might be explained by water incorporation into the lattice acting destabilizing,[18] as discussed above. In this work virtually no nucleation of magnesite occurred for sample A while some magnesite is present in the other samples, see Fig. 2. However, in the oxymagnesite forming samples (mainly in the highest RH samples C, D and E) the amount of oxymagnesite does not seem to vary significantly between the samples based on the intensity in the X-ray diffractograms see Fig. 2. Thus, it may be assumed that oxymagnesite is more easily crystallized than magnesite. However, oxymagnesite is formed from a decomposition reaction during the thermal treatment while for magnesite nucleation the thermal treatment mainly acts as an aid for crystallization. Why oxymagnesite is easier to crystallize than magnesite is not known; but knowing that water facilitates crystallization[33, 34] and assuming that oxymagnesite is formed from a "nesquehonite-like" AMC phase it can be argued that 48 hours is enough to induce migration of the atoms into this "nesquehonite-like" structure (detectable nesquehonite is formed only after several weeks of hydrolysis). In contrast, for nucleation of magnesite after thermal treatment of AMC during 48 hours of hydrolysis was not enough. Since it here can be argued that oxymagnesite is more easily crystallized than magnesite it is interesting that, to the best of our knowledge, there exist no reports about the presence of oxymagnesite in nature, which undisputedly raises questions about its stability. A stable, easily crystallized magnesium carbonate compound seems unlikely not to exist in nature. To examine the stability of oxymagnesite a TGA analysis of sample E was performed, the result can be seen in Fig. 6. Evidently, oxymagnesite decomposes at around 400 ºC, which is below the decomposition temperature of magnesite. Hence, oxymagnesite appears to be less stable then magnesite.

In Fig. 2 it can be seen that sample A was almost entirely amorphous with some broad peaks from periclase present in the diffractogram likely due to partial decomposition of the carbonate. Sample B formed a mixture of amorphous phase(s), magnesite and traces of oxymagnesite after the thermal treatment while sample C and D formed mainly oxymagnesite with some magnesite and periclase present in the sample as well. The broad peaks from periclase were present in all the samples that were placed farther away from the middle of the furnace while the samples that were placed in the middle, *i.e.* sample B and E did not show any periclase peaks in the diffractogram. Consequently, it is anticipated that the reason for this is differences in temperature within the furnace especially since 300 °C is close to the temperature at which carbonate decomposition starts; a shift towards higher temperatures can be assumed to result in partial decomposition of the carbonate.

Characterization of oxymagnesite.

Sample E, which was hydrolyzed with liquid water, contained only one detectable crystalline phase; *viz.* oxymagnesite in addition to an amorphous phase as can be seen in Fig. 2 and

Fig. 7. The full pattern refinement of the powder X-ray diffractogram of sample E shows a good fit to the structure reported in Watabe et al.[7] except for the O-atom occupancies, see Fig. 7. The obtained oxymagnesite crystals were also examined with SAED and the obtained patterns are in good agreement with the XRD data. The morphology of oxymagnesite, observed both by SEM and TEM in this work shows that the oxymagnesite crystals clearly differ from the crystals of magnesite, see Fig. 5. These findings support the conclusion previously drawn by Hladky[6] that oxymagnesite is indeed a new phase and not a mixture of MgO and $MgCO_3$. Another interesting feature that can be seen in the SEM image in Fig. 5a is that the amorphous material surrounding the oxymagnesite crystals appears to be porous. The reason for the porosity has not been examined further but it may be explained by the rapid heat treatment for this sample type where no ramping time was used; the samples were subjected to 300 °C directly from RT. During this thermal treatment water of a mass corresponding to ~10 wt% of the sample (based on TGA data) was being removed. The fast water removal may have created the pores.

Conclusions

In this work oxymagnesite, $2MgCO_3 \cdot MgO$ has been synthesized in a controlled way by thermal treatment of hydrated AMC, $MgCO_3 \cdot xH_2O$. The AMC was synthesized from $Mg(OCH_3)_2$ under pressurized CO_2 in order to first form $Mg(OCO)(OCH_3)_2$, that in the following reaction step is hydrolyzed to form AMC. By varying the relative humidity during hydrolysis the structural arrangement within the AMC varied so that either oxymagnesite and/or magnesite formed upon the thermal treatment. When RHs higher than a certain threshold were used for hydrolysis the subsequent thermal treatment resulted in the formation of oxymagnesite whereas lower RHs did not. In our work this threshold was found to lie in the interval between 11 and 52% RH. It is speculated that the arrangement within the structure and not necessarily the amount of water is the pivotal factor for the formation of oxymagnesite. The peculiar phase oxymagnesite has only been reported a handful of times previously. This study is the first in which the synthesis of oxymagnesite has been controlled and also the first study where SEM and TEM images of its crystals have been showed. The results presented herein open up for the possibility to control the phase composition(s) of magnesium carbonates after thermal treatment by controlling the amorphous magnesium carbonate prior to thermal treatment.

Addresses

aDivision for Nanotechnology and Functional Materials, Department of Engineering Sciences, The Ångström Laboratory, Uppsala University, Box 534, SE-751 21 Uppsala, Sweden. Email: maria.stromme@angstrom.uu.se; Tel: +46 (0)18 471 7231

bDepartment of Chemistry - Ångström Laboratory, Uppsala University, Box 534, SE-751 21 Uppsala, Sweden

cLaboratoire Interdisciplinaire Carnot de Bourgogne, UMR 6303 CNRS – Université de Bourgogne, 9 Av. A. Savary, BP 47870, 21078 Dijon Cedex, France

References

1. J. Forsgren, S. Frykstrand, K. Grandfield, A. Mihranyan and M. Strømme, *PLoS ONE*, 2013, **8**, e68486.
2. S. Frykstrand, J. Forsgren, A. Mihranyan and M. Strømme, *Micropor, Mesopor. Mat.*, 2014, **190**, 99.
3. I. Pochard, S. Frykstrand, O. Ahlstrom, J. Forsgren and M. Strømme, *J. Appl. Phys.*, 2014, **115**, 044306.
4. P. Zhang, J. Forsgren and M. Strømme, *Int J Pharm*, 2014, **472**, 185.
5. P. Ballirano, C. De Vito, V. Ferrini and S. Mignardi, *J. Hazard. Mater.*, 2010, **178**, 522.
6. G. Hladky, *Neues Jahrb. Mineral., Monatsh.*, 1975, 115.
7. K. Watabe, Y. Seto and H. Miura, *J. Comput. Chem. Jpn.*, 2009, **8**, 179.
8. D. S. Shlyapnikov, E. K. Shtern, I. G. Demchuk and L. A. Sherstobitova, *Dokl. Akad. Nauk SSSR*, 1982, **265**, 701.
9. J. Fagerlund, J. Highfield and R. Zevenhoven, *R. Soc. Chem. Adv.*, 2012, **2**, 10380.
10. J. Fagerlund, E. Nduagu, I. Romão and R. Zevenhoven, *Energy*, 2012, **41**, 184.
11. T. Kornprobst and J. Plank, *J. Non-Cryst. Solids*, 2013, **361**, 100.
12. K. Sandengen, L. O. Josang and B. Kaasa, *Ind. Eng. Chem. Res.*, 2008, **47**, 1002.
13. H. Rietveld, *J. Appl. Crystallogr,*, 1969, **2**, 65.
14. J. Rodríguez-Carvajal, in *Satellite meeting on powder diffraction of the XV IUCr congress*, 1992, p. 127.
15. P. Stadelmann, *JEMS Java Electron Microscopy Software*, (2004).
16. W. White, *Environ. Geol.*, 1997, **30**, 46.
17. J. Xu, C. Yan, F. Zhang, H. Konishi, H. Xu and H. H. Teng, *PNAS*, 2013, **110**, 17750.
18. A. Botha and C. A. Strydom, *Journal of Thermal Analysis and Calorimetry*, 2003, **71**, 987.
19. J. C. Deelman, *Neues Jb. Miner. Monat.*, 1999, **7**, 289.
20. J. C. Deelman, *Chem. Erde*, 2001, **61**, 224.
21. C. Berg, M. Beyer, U. Achatz, S. Joos, G. Niedner-Schatteburg and V. E. Bondybey, *Chem. Phys.*, 1998, **239**, 379.
22. F. L. Sayles and W. S. Fyfe, *Geochim. Cosmochim. Ac.*, 1973, **37**, 87.
23. D. D. Tommaso and N. H. de Leeuw, *Phys. Chem. Chem. Phys.*, 2010, **12**, 894.
24. Y. Yang, N. Sahai, C. S. Romanek and S. Chakraborty, *Geochim. Cosmochim. Ac.*, 2012, **88**, 77.
25. D. Jiao, C. King, A. Grossfield, T. A. Darden and P. Ren, *J. Phys. Chem. B*, 2006, **110**, 18553.
26. P. E. Barran, N. R. Walker and A. J. Stace, *J. Chem. Phys.*, 2000, **112**, 6173.
27. F. C. Lightstone, E. Schwegler, R. Q. Hood, F. Gygi and G. Galli, *Chem. Phys. Lett.*, 2001, **343**, 549.
28. C. L. Christ and P. B. Hostetler, *Am. J. Sci.*, 1970, **268**, 439.
29. G. H. Wolf, A. V. Chizmeshya, J. Diefenbacher and M. J. McKelvy, *Environ. Sci. Technol.*, 2004, **38**, 932.
30. D. E. Giammar, R. G. Bruant Jr and C. A. Peters, *Chem. Geol.*, 2005, **217**, 257.

31. M. Hänchen, V. Prigiobbe, R. Baciocchi and M. Mazzotti, *Chem. Eng. Sci.*, 2008, **63**, 1012.

32. A. P. A. Anjos, A. Sifeddine, C. J. Sanders and S. R. Patchineelam, *Carbonate. Evaporite.*, 2011, **26**, 213.

33. S. J. Teichner, G. A. Nicolaon, M. A. Vicarini and G. E. E. Gardes, *Adv. Colloid. Interfac.*, 1976, **5**, 245.

34. R. M. Dell and S. W. Weller, *T. Faraday Soc.*, 1959, **55**, 2203.
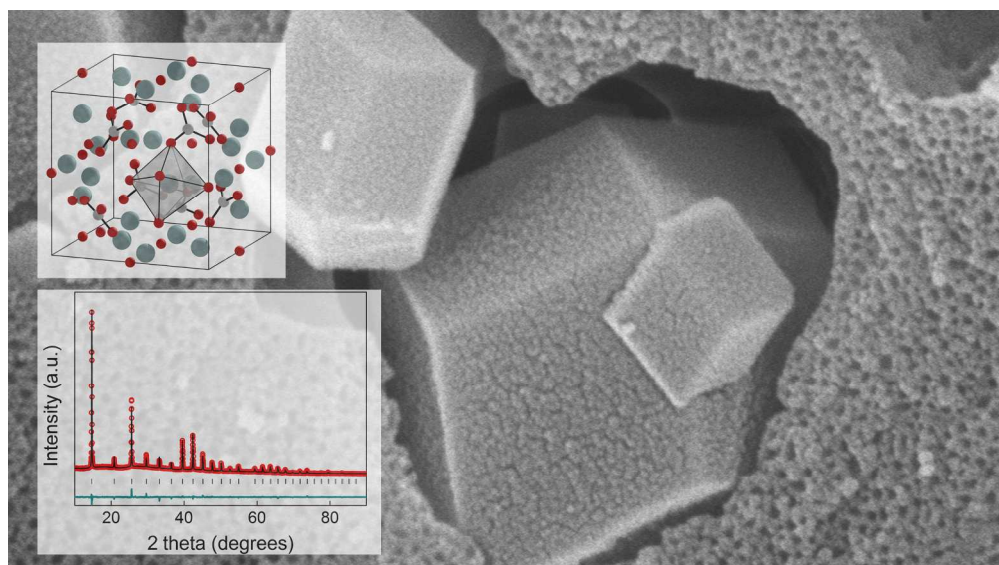
The first electron microscopy images of the peculiar oxymagnesite crystal are presented along with synthesis description and crystallographic data.